An FM/CW Method for the Measurements of Time Delays of Large Cassegrain Antennas

T. Y. Otoshi
Radio Frequency and Microwave Subsystems Section

An FM/CW measurement technique, which utilizes the time domain principle, was developed to measure the time delays of large Cassegrain antennas. Measured primary path delays of 60 ns (or greater) typically agreed with calculated delays to within 3 ns. Multipath sources generated within the antenna optics region have been identified.

I. Introduction

Large Cassegrain microwave antennas are currently being used as the ground station terminal in most deep space communication systems. At some stations the same antenna is also used as part of a ranging system to obtain spacecraft-to-Earth range data needed for spacecraft navigation. To determine the true range of the spacecraft from the ground station location, time delay calibrations must be performed on the microwave antenna as well as on the ground station equipment (Ref. 1). Accurate determination of the signal delay time through the antenna is also critical to the success of clock synchronization experiments using Very Long Baseline Interferometry (VLBI) techniques (Ref. 2).

Extensive experimental work has been done in the JPL/NASA Deep Space Network (DSN) to develop a simple but accurate method for the measurement of antenna time delay of a large Cassegrain antenna. Most of the methods investigated were found to be susceptible to large errors caused by multipath signals generated within the region between the main reflector and subreflector surfaces. This paper describes a time domain measurement technique which enables accurate measurement of the primary signal delay time without interference from major multipath signals. The following sections of this paper present discussions of the multipath problems associated with antenna time delay calibrations, FM/CW theory and instrumentation, and experimental data obtained on 64- and 26-m antennas.

II. Antenna Delay Calibration Problems

Figure 1 shows a typical 64-m-diameter Cassegrain antenna used in the DSN. This particular antenna is equipped with a reflex-dichroic system to enable simultaneous reception of S- and X-band frequencies. The feedcones are aluminum housings that contain feed assemblies as well as transmitter and receiver equipment. A signal originating from the far-field is collected by the parabolic reflector, reflected to the subreflector, re-reflected, and arrives at the receive horn via the ray paths of the dual-band system.

The calibration problem is to determine the antenna delay, which for purposes of this paper shall be defined as the time it takes for the illuminating signal to propagate from a designated reference plane (such as the antenna focal plane) to a designated output port of the receive horn assembly. It should be pointed out that another definition of antenna delay, which does not include the waveguide delays of the feed horn assembly, was given previously in Ref. 3.

A method that has been used for the calibration of antenna delay (as defined in this paper) is depicted in Fig. 2. The horn on the dish surface can be viewed as one "cell or element" of the total signal collected by the many cells of the parabolic reflector. The calibration procedure is to inject a signal into the dish-mounted horn that is pointed toward the subreflector. A time delay measurement is made between the input port of the transmit horn (on dish surface) and a designated output port in the receive system horn assembly. A theoretical constant is then added to the measured value to artificially move the signal input reference plane from the dish location to the paraboloid focal plane. In the ideal case, the corrected measured delay value would be the same as the antenna delay for the entire Cassegrain antenna. The basic assumption is made that all signals follow geometric optics (GO) ray paths so that they all have the same delay (path length) from the paraboloid focal plane to the system feed horn focal point.

In practice numerous factors such as blockage, mechanical supports, imperfect reflector surfaces, mechanical distortions, and defocusing cause departure from the ideal Cassegrain antenna. Furthermore, two known types of multipath signals are generated within the antenna optics media of practical Cassegrain antennas. The first type is caused by a portion of the illuminating plane wave signal becoming blocked by the large subreflector and subreflector support struts. Diffraction around the edges of the subreflector and struts will occur and a portion of these diffracted fields propagates directly into the receive horn. Another type of multipath phenomenon that occurs is that generated by unwanted multiple reflections between the subreflector and feedcone surfaces (Fig. 3).

In order to determine the magnitude of deviations from ideal antenna time delay caused by the multipath phenomenon, far-field time delay experiments were performed on DSN 64-m antennas. The far-field signals were ranging signals provided by Viking spacecraft at S-band and Voyager spacecraft at X-band. From the test data (Ref. 4) it was found that multiple-reflection type multipath signals produced maximum errors of ±3 ns when a ranging modulation frequency of 500 kHz was used. These errors were produced by multipath signals at least 40 to 46 dB down from the primary signal for the 64-m antenna. These experimental observations were also supported by results of a far-field theoretical study performed by Rusch (Ref. 5). In a separate study, a cursory theoretical analysis showed that diffractions from the subreflector edge and struts would produce time delay errors smaller than those produced by multiple reflections. Although these far-field experiments and analyses provided valuable information on the effects of multipath errors on the total Cassegrain antenna received signal, there was still a need for an accurate method to calibrate *absolute* antenna delay.

During the period of 1975-1976, several methods were investigated as possible ways to calibrate absolute antenna and ground station delays. Far-field methods for calibrating absolute antenna delays were shown by Sato in Ref. 6 to be expensive, and it was concluded that the necessary technology and equipment would take considerable effort and time to develop. As a parallel effort to find different methods to calibrate antenna delays, a separate theoretical study was made by A. Cha (Ref. 7) to investigate near-field methods as well. The results from this theoretical study showed that if multipath effects were negligible, then far-field absolute antenna delays for 26-m and 64-m DSN-type antennas could be determined to a 1 or 2 ns accuracy level with the horn-on-dish calibration method. He found that for propagation paths between the main reflector surface and the system feed horn, the delays computed by the geometric theory of diffraction (GTD) agreed with the delays computed by the geometric optics theory to better than 1 ns. It was concluded from this study that further efforts should be directed towards developing the horn-on-dish method for absolute antenna delay calibrations.

A major problem discovered after extensive testing with the horn-on-dish method was the generation of new multipath signals by the calibration geometry itself. Very often the antenna pattern of the transmit horn (on dish surface) will have insufficient directivity and high side-lobes. Therefore, the calibration signal will not only follow the primary ray path, but will also follow other ray paths due to unintentional illuminations of the struts and side of the feedcone housings. When conventional time delay measurement methods (modulation and phase-slope methods) were employed to measure time delays, it was found that the accuracy of results was seriously degraded by multipath signals and critically dependent upon (1) the directivity of the calibration horn used, (2) the selected location of this horn on the dish surface, and (3) the bandwidth of the measurement.

After experiencing considerable problems with conventional techniques, a solution was made possible by a diagnostic instrument that utilized the FM/CW technique based on the time domain principle. Not only did it become possible to isolate and make accurate measurement of primary path time delays, but it also became possible to positively identify the

existence and origins of multipath signals associated with any calibration configuration.

III. FM/CW Theory and Instrumentation

The instrument used for making antenna time delay measurements is a Scientific-Atlanta Series 1691 Fault Locator (Ref. 8), which is an FM/CW radar system (Ref. 9) that can be operated at any center frequency in the microwave range from 1.7 to 12.4 GHz with sweep bandwidths varying from 40 to 100 MHz. The instrument is intended primarily to be used as a diagnostic tool to locate various discontinuities in a microwave transmission line and measure the magnitude of return losses as functions of the distances (range) to the discontinuities. For the test results of this paper, however, the instrument was modified to operate in a "transmission" or one-way mode rather than in the normal return loss or bistatic radar mode. Figure 4 shows the instrument with the modifications. In this transmission mode, the measured delays can be compared to path lengths obtained from antenna mechanical drawings, and the measured magnitudes of the received signals can be compared to those calculable from the Friis transmission formula (Ref. 10).

Figure 5 is a functional block diagram of the instrumentation. A sample of the oscillator output signal is fed to the local oscillator input of the mixer. The remainder of the signal is fed to the transmit antenna. Figure 6 shows that the oscillator output frequency is changed in a sawtooth manner, over the sweep bandwidth $2\Delta F$, around the center frequency F_0. Thus, data is gathered over the $F_0 \pm \Delta F$ frequency range. The solid line represents the oscillator output (transmit signal) as a function of time while the dashed line represents the received signal. Only one of the receive signals is shown in Fig. 6 in order to illustrate the basic principle of operation. The basic relationship for this instrumentation as derived by the proportional triangle relationships in Fig. 6 is

$$t_g = f_d \left(\frac{T}{2\Delta F}\right) \tag{1}$$

where t_g is the propagation time or time delay of interest, f_d is the difference frequency, T is the sawtooth modulation period, and ΔF is one-half the sweep bandwidth. If d is defined as the path length from transmit antenna to the receive antenna, and the group velocity v_g of the signal in the propagation media is known, then the path length can be computed from

$$d = v_g f_d \left(\frac{T}{2\Delta F}\right) \tag{2}$$

If f_d is fixed, then the path length is inversely related to the oscillator modulation rate, $2\Delta F/T$.

The mixer (see Fig. 5) produces an output signal that contains a difference frequency f_d for each received signal of different path length. The control unit of this instrument varies the sweep bandwidth and causes the distance readout to indicate a focus distance d when the difference frequency produced by the received signal is equal to 5 kHz and has an integer number of cycles in the sawtooth period T shown in Fig. 6. The narrowband IF amplifier rejects all the other received "target" signals and feeds this signal into the log converter which drives the signal magnitude meter. Since the distance indicated by this instrument is calibrated for an equivalent bistatic radar configuration, the "target" distance readings are multiplied by 2 when the instrument is modified for use for the one-way or transmission mode.

It is beyond the scope of this article to present further details of the instrument. The mathematical relationships of the FM/CW theory can be found in Refs. 8 and 9 and additional details on the Fault Locator design can be found in Scientific-Atlanta Fault Locator instrument manuals. It is sufficient for purposes of this article to state that when the Fault Locator is focused at a distance in the vicinity of a single "target" response, the signal magnitude meter and plot recorder output displays a response of the form

$$R_{dB} = 20 \log_{10} \left| \frac{A \sin(\pi u)}{\pi u (1 - u^2)} \right| \tag{3}$$

where A is the target signal amplitude normalized to a reference signal level that was initially established with a zero dB set control. In Eq. (3), u is a variable that is directly related to sweep bandwidth and to the difference between the focus distance and the "target" distance. A peak response is observed when u becomes zero as a result of adjusting the focus distance to be equal to the "target" distance. The measured propagation path length at this peak response is the distance between the transmit and receive antennas, provided that the instrumentation has been adjusted to indicate zero when there is no separation between the antennas.

Increasing the sweep bandwidth narrows the width of the response and improves the resolution of the delay measurement. However, the sweep bandwidth cannot be controlled in the commercial units due to automatic setting of the sweep bandwidth to a value (between 40 to 100 MHz) depending upon the target range.

Further work has since been done by the Howland Company of Atlanta, Ga., to enable manual setting of sweep band-

widths, increasing sweep bandwidths up to 300 MHz, and increase the range of transmission mode measurements from 1500 to 30,000 ns (Ref. 11).

IV. Measurement of Primary Path Delays

Figure 7 shows a block diagram of the test setup that was used to measure time delays of primary and secondary signals within the antenna optics media of a Cassegrain antenna. The modified Fault Locator instrument and recorder were placed inside the S-band Cassegrain feedcone close to the base of the receive system feed horn. A short 1.8-m (6-ft) cable was connected between the receive system output port and the Fault Locator "receive" port. Then a 30.48-m (100-ft) low-loss flexible cable with amplifiers in series was connected between the Fault Locator signal output port and the transmit horn (standard gain type) located on the dish surface as shown in Fig. 7. The amplifiers were of the compact solid-state type and provided a combined gain of about 40 dB to compensate for the airpath loss between the transmit horn and the system receive horn. All components including test cables and amplifiers were pretested and selected for constant group delay over a wide bandwidth and also for group and phase delay stability with mechanical flexing and temperature changes.

The basic measurement technique is described as follows. A measurement is first made of the total system delay. The total system for this test configuration consists of the transmit horn, the airpath, receive horn feed assembly, cables, amplifiers, and the Fault Locator instrument. Then a reference measurement is made by disconnecting (1) the cable at the transmit horn and (2) the cable at the receive system output port, and then connecting the two cables (with amplifiers) together with a 40-dB coaxial pad inserted in between. The 40-dB pad value was used to attenuate the increase in signal level due to removal of the airpath loss which was in the total system measurement. Subtraction of the reference measurement from the total system measurement, with small corrections applied for the delay of the transmit horn and 40-dB pad, resulted in the primary path delay value of interest.

To make the actual measurement of primary path delay with the Fault Locator instrument, the dial on the Fault Locator is manually adjusted to a setting that provides maximum received signal. The path length is directly read off the dial in units of feet and multiplied by 2 for transmission mode measurements. For these antenna delay measurements, the resolution of the measurements was improved to about 3.1 cm (0.1 ft) by incorporating more sensitive indicators into the instrument. All measured values were later converted from path length in feet into time delay in ns.

Measurements through the use of the described test procedure were made on the 64-m antenna at S- and X-band frequencies with the transmit horn at the different test locations shown in Fig. 8(a). With the exception of Location 5, all other locations were on the dish surface. Location 5 was adjacent to and on the same level as the tricone support platform (see Fig. 2) and therefore physically closer to the subreflector than the other locations. Table 1 presents a summary of the measured primary path delays and deviations from calculated values. The primary path delays are absolute time delays for a signal propagating from the horn-on-dish location to the output flange of the receive system horn assembly via the Cassegrain system primary ray paths. The calculated primary path delay values in Table 1 were based on physical dimensions for the airpath and group velocities of various waveguides in the receive horn feed assembly. It can be seen in Table 1 that all of the measured primary path delays were greater than 100 ns and typically agreed with calculated values to within 3 ns. About 1 ns of the disagreement is attributed to uncertainties in the calculated values. The results of the calculated feedhorn assembly delays are tabulated in Ref. 12.

Table 2 shows the results of similar measurements of primary path delays performed on a 26-m DSN antenna. The experimental setup was similar to that for the 64-m antenna except that a shorter cable was used to connect the Fault Locator to the transmit horn on the dish surface at the different locations shown in Fig. 8(b). As may be seen in Table 2, the measured primary path delays for the 26-m antenna were between 60 and 75 ns. The agreement between measured and calculated delays was typically within 3 ns. The calculated delays were again based on physical dimensions from antenna drawings and group velocities of the waveguide components of the feed assembly.

The purpose of comparing calculated and measured values is to provide a basis for evaluating the accuracy of antenna delay measurements when performed with the FM/CW technique. Previous attempts to measure the same delay paths with other measurement techniques led to disagreement with calculated values as large as 20 to 30 ns in some cases (Ref. 13). The order-of-magnitude improvement of accuracy obtained with the FM/CW method is basically due to the time domain principle and large sweep bandwidths of 40 to 100 MHz which enable isolation of the primary signal from the secondary signals during the measurement.

For both the 64- and 26-m antennas, it was fortunate that the feed assembly consisted of relatively simple components whose delay could be calculated. In the DSN, there are more complex Cassegrain feed systems such as ones with a monopulse feed whose delay is difficult to calculate accurately. For such complex feed systems, a relatively simple and direct mea-

surement of antenna delay with the FM/CW instrument can now be performed.

V. Identifications of Multipath Sources

Identification of multipath signals is easily accomplished by means of a time domain recording such as the plot shown in Fig. 9. With the horn-on-dish calibration setup discussed in the previous section, this recording was made automatically with a push of a button on the Fault Locator instrument. The plot not only displays the primary signal response but the responses of all other secondary signals. The horizontal scale of Fig. 9 was corrected so that it shows absolute path length in the transmission mode. The multiple bounce surfaces for multipath sources labeled a, b, and c in Fig. 9 are identified in Fig. 3. Since multiple reflection signals travel longer distances to arrive at the receive horn, they appear on the plot at path lengths longer than the primary signal. It is of significance to note that the relative magnitudes of the largest multipath signals are approximately 20 dB down from the primary signal. Also note that the relative position of the Cassegrain subreflector has a large effect on the magnitudes of the multipath signals, but very little effect on the magnitude of the primary signal. Movement of the subreflector and observations of the changes of the sidelobe structures provided a means for verifying that the sidelobe responses were due to multipath signals and were not part of the normal $(\sin \pi u)/(\pi u)$ type response of the primary signal (See Eq. 3).

Similar types of recordings were obtained at all of the horn locations and microwave frequencies shown tabulated in Table 1. In order to verify that the multipath sources were correctly identified, a 2-ft-square absorbing sheet was systematically placed at multiple reflection points such as at the a, b, c locations shown in Fig. 3. If the multiple reflection point of the multipath source was correctly located, a new recording would show a decrease of 1 to 2 dB in the response of the multipath signal being investigated. This simple procedure was used to confirm the location of the multiple reflection surfaces on the antenna structure.

Figure 10 shows similar types of recordings taken on a 26-m DSN antenna. Figure 10(a) is a plot taken with the transmit horn near the side of the feedcone housing. At this horn location, the strength of the largest multipath signal was about 28 dB down from the peak response of the primary signal. Figure 10(b) is a plot taken with the transmit horn placed near the outer edge of the reflector surface. It is interesting to note that at this location the dominant multipath signal has increased relative to the primary signal.

Recordings taken for various horn locations on the reflector surface proved to be very useful for providing insight into the mechanism of the generation of multipath signals and understanding of multipath phenomena for the far-field signal case as well. The diagnostics work with the Fault Locator confirmed that the horn-on-dish method would be very susceptible to large errors if used with the DSN ranging system, which operates with a small modulation bandwidth of 500 kHz. This work led to the development of a "translator method," which is described in Ref. 1 and is a new method now being used throughout the DSN to calibrate ground station delays for ranging systems.

VI. Conclusions

The FM/CW technique in conjunction with the horn-on-dish configuration proved to be the most rapid, convenient, and accurate method for calibrating absolute time delays for a large antenna. The work discussed in this article was performed in 1977 and the results at that time represented a major improvement in achievable accuracies in the measurements of signal path delays within the antenna optics media of large Cassegrain antennas. Through the use of a commercially available FM/CW instrument, accuracies of about 3 ns were obtained on measurement of primary path delays of 60 ns or greater.

The FM/CW instrumentation was invaluable as a diagnostics tool and facilitated increased understanding of the mechanisms of multipath signal generation within the antenna optics media. Time domain plots enabled positive identifications of major multipath signals that could be deleterious to accuracy of antenna time delay calibrations. A beneficial outcome of this work is that attention is now being focused on minimizing multipath signals on future DSN antennas to be used for ranging and VLBI applications.

Acknowledgment

The author thanks R. B. Lyon and M. Franco of JPL for their assistance in setting up the experiment and collecting the data. A. Ray Howland, president of the Howland Co. in Atlanta, Ga., suggested the use of the Fault Locator instrument to locate multipath sources within the antenna propagation paths. He also consulted on the instrument modification and assisted with the measurements and interpretation of the test data.

References

1. Komarek, T., and Otoshi, T. Y., "Terminology of Ranging Measurements and DSS Calibrations," in *The Deep Space Network Progress Report 42-36*, pp. 35-40, Jet Propulsion Laboratory, Pasadena, Calif., Dec. 15, 1976.

2. Otoshi, T. Y., "Definition of Antenna Microwave Time Delay for VLBI Clock Synchronization," in *The Deep Space Network Progress Report 42-49*, pp. 45-56, Jet Propulsion Laboratory, Pasadena, Calif., Feb. 15, 1979.

3. Cha, A. G., Rusch, W. V. T., and Otoshi, T. Y., "Microwave Delay Characteristics of Cassegrainian Antennas," *IEEE Trans. Ant. Prop.*, Vol. AP-26, pp. 860-865, Nov. 1978.

4. Otoshi, T. Y., and Brunn, D. L., "Multipath Tests on 64-m Antenna Using the Viking Orbiter -1 and -2 Spacecraft as Far-Field Illuminators," in *The Deep Space Network Progress Report 42-31*, pp. 41-49, Jet Propulsion Laboratory, Pasadena, Calif., Feb. 15, 1976.

5. Otoshi, T. Y., and Rusch, W. V. T., "Multipath Effects on the Time Delays of Microwave Cassegrainian Antennas," *AP-S International Symposium Digest – Antennas and Propagation*, Vol. II, 80 CH 1557-8AP, pp. 457-460, June 1980.

6. Sato, T., "Feasibility Study of Far-Field Methods for Calibrating Station Delays: An Interim Report," in *The Deep Space Network Progress Report 42-41*, pp. 51-56, Jet Propulsion Laboratory, Pasadena, Calif., Oct. 15, 1977.

7. Cha, A. G., private communication, June 1977.

8. Howland, A. Ray, "Testing Microwave Transmission Lines," *IEEE S-MTT Conference Digest 1974*, pp. 258-260, June 1974.

9. Ismail, M. A-E. W., "A Study of the Double Modulated F. M. Radar," Thesis presented to Swiss Federal Institute of Technology, Zurich, 1955.

10. Kraus, J. D., *Antennas*, McGraw-Hill, New York, p. 54, 1950.

11. Howland, A. R., "Modified Fault Locator Evaluation," *Howland Company Report HC-685115*, Howland Company, Atlanta, Ga. Nov. 14, 1978.

12. Otoshi, T. Y., Wallace, K. B., and Lyon, R. B., "Dual Coupler Configuration at DSS 14 for the Voyager Era," in *The Deep Space Network Progress Report 42-42*, pp. 184-190, Jet Propulsion Laboratory, Pasadena, Calif., Dec. 15, 1977.

13. Otoshi, T. Y., "A Collection of Articles on S/X-Band Experiment Zero Delay Ranging Tests," *Technical Memorandum 33-747*, Vol. 1, Jet Propulsion Laboratory, Pasadena, Calif., p. 123, Nov. 1975.

Table 1. Results of 64-m antenna primary path delay measurements

Horn-on-dish location	System horn polarization	Test frequency, GHz	Measured delay, ns	Measured minus calculated delay, ns
1	LP	2.113	172.3	0.5
2	LP	2.113	164.7	1.9
2	RCP	2.113	164.1	1.3
3	LP	2.113	159.0	3.5
3	RCP	2.113	157.1	1.6
4	RCP	2.113	166.4	3.7
5	LP	2.113	129.3	−0.8
5	RCP	2.113	132.2	2.0
1	LP	2.295	169.0	−0.2
1	RCP	2.295	170.1	0.9
3	LP	2.295	154.9	2.1
3	RCP	2.295	154.9	2.1
4	RCP	2.295	160.0	−0.1
5	LP	2.295	129.3	1.7
5	RCP	2.295	126.7	−0.9
1	RCP	8.415	143.4	0.8
2	RCP	8.415	136.8	3.1
3	RCP	8.415	130.1	3.6
4	RCP	8.415	135.4	1.7
5	RCP	8.415	100.9	−0.3

Table 2. Results of 26-m antenna primary path delay measurements

Horn-on-dish location	System horn polarization	Test frequency, GHz	Measured delay, ns	Measured minus calculated delay, ns
1	LP	2.113	62.4	0.4
1	RCP	2.113	65.4	3.5
2	LP	2.113	72.2	0.4
2	RCP	2.113	72.5	0.7
1	LP	2.295	63.0	1.3
1	RCP	2.295	62.6	0.9
2	LP	2.295	74.2	2.7
2	RCP	2.295	74.9	3.4
3	LP	2.295	68.1	−1.2

Fig. 1. DSN 64-m Cassegrain antenna at Goldstone, Calif.

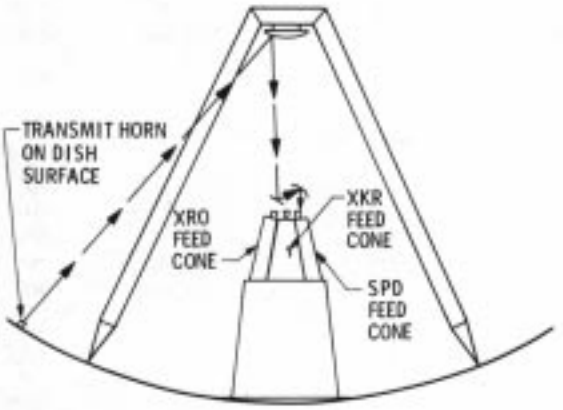

Fig. 2. Principal calibration system propagation path on DSN 64-m antenna

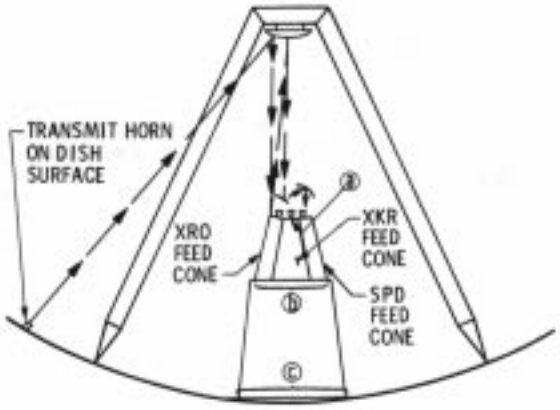

Fig. 3. A secondary propagation path on DSN 64-m antenna

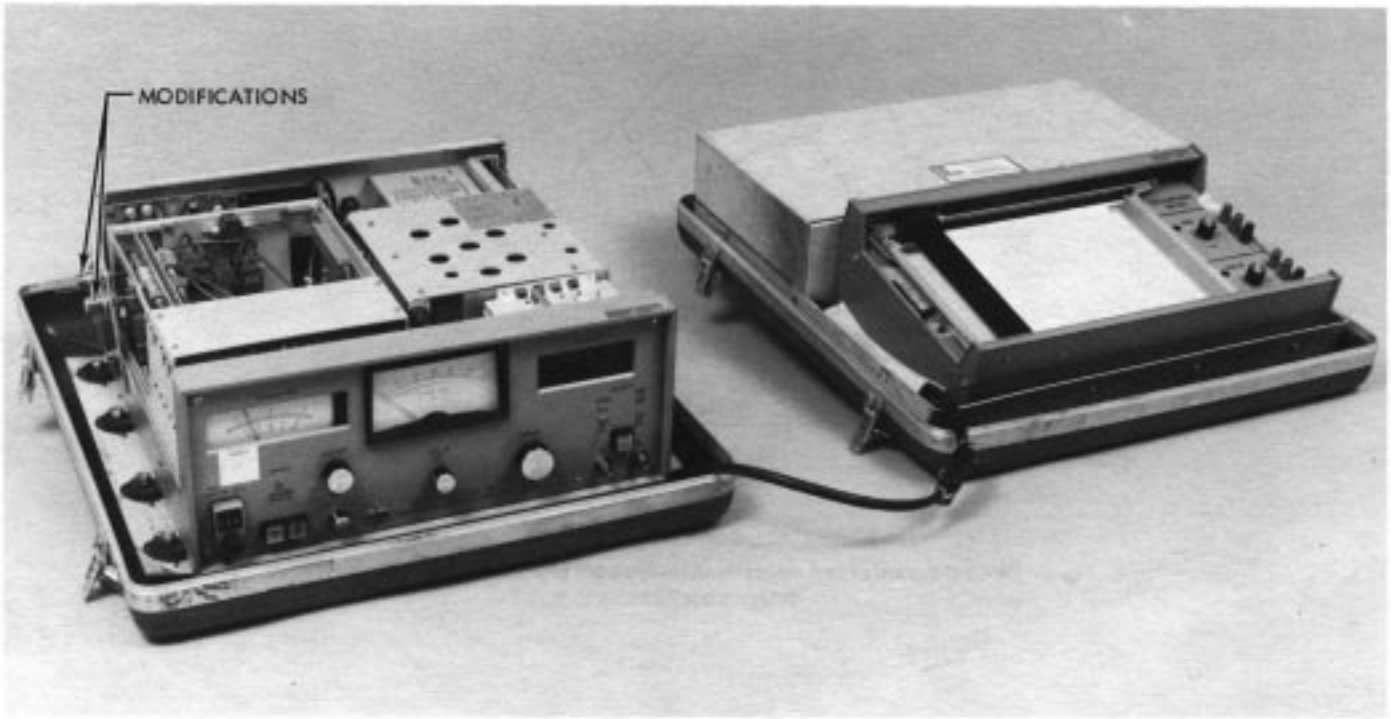

Fig. 4. Modified Fault Locator and recorder

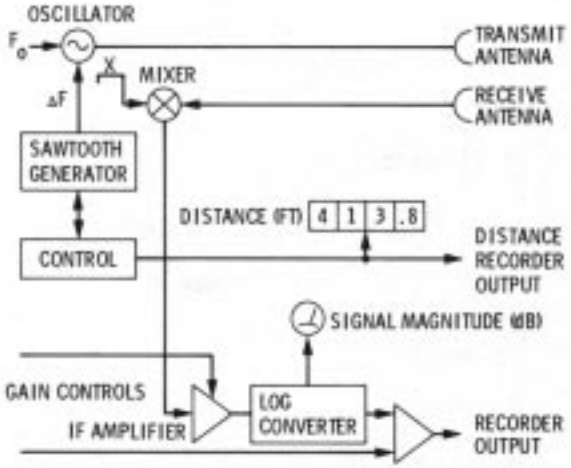

Fig. 5. Block diagram of FM/CW instrumentation

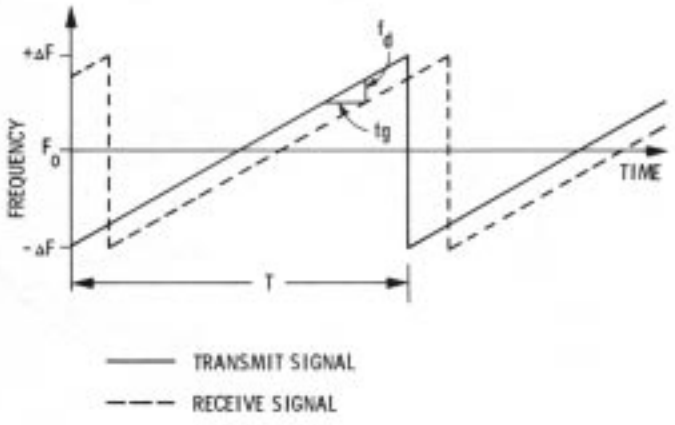

Fig. 6. FM/CW signal relationship

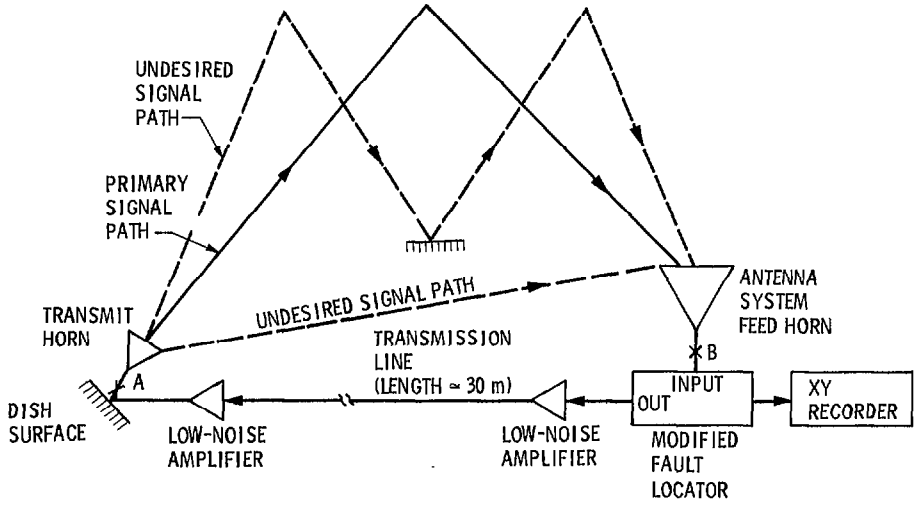

Fig. 7. Block diagram of test setup for measurement of primary and multipath signal delays from Points A to B

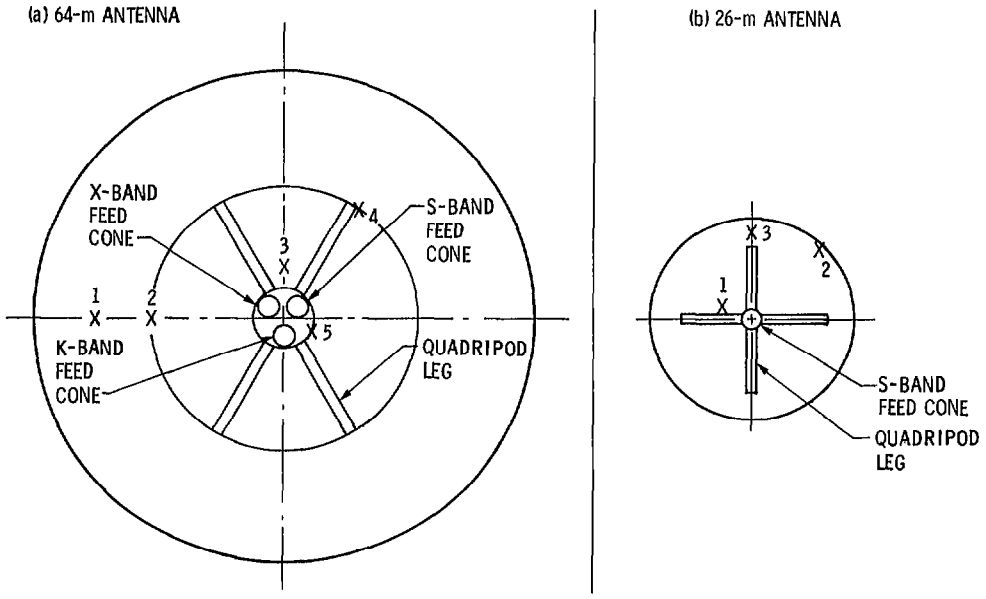

Fig. 8. Transmit horn locations for tests on (a) 64-m antenna and (b) 26-m antenna

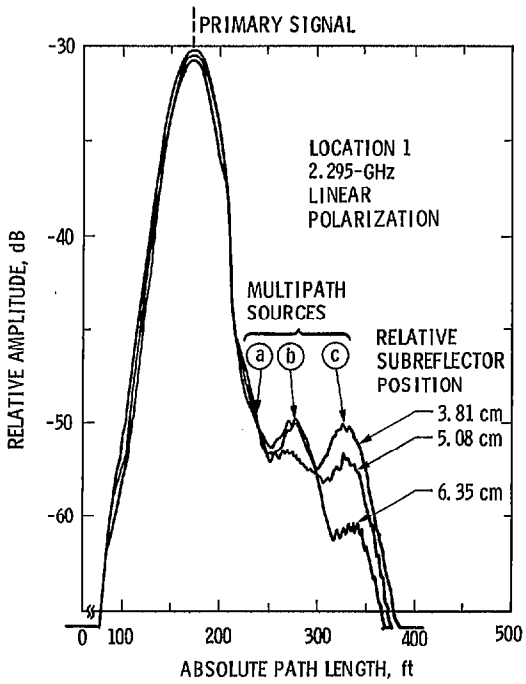

Fig. 9. Sample recording of path lengths and relative signal magnitudes of primary and secondary signals for a 64-m antenna test setup. The instrument records path length in units of feet and therefore it is not meaningful to convert the horizontal scale to metric units.

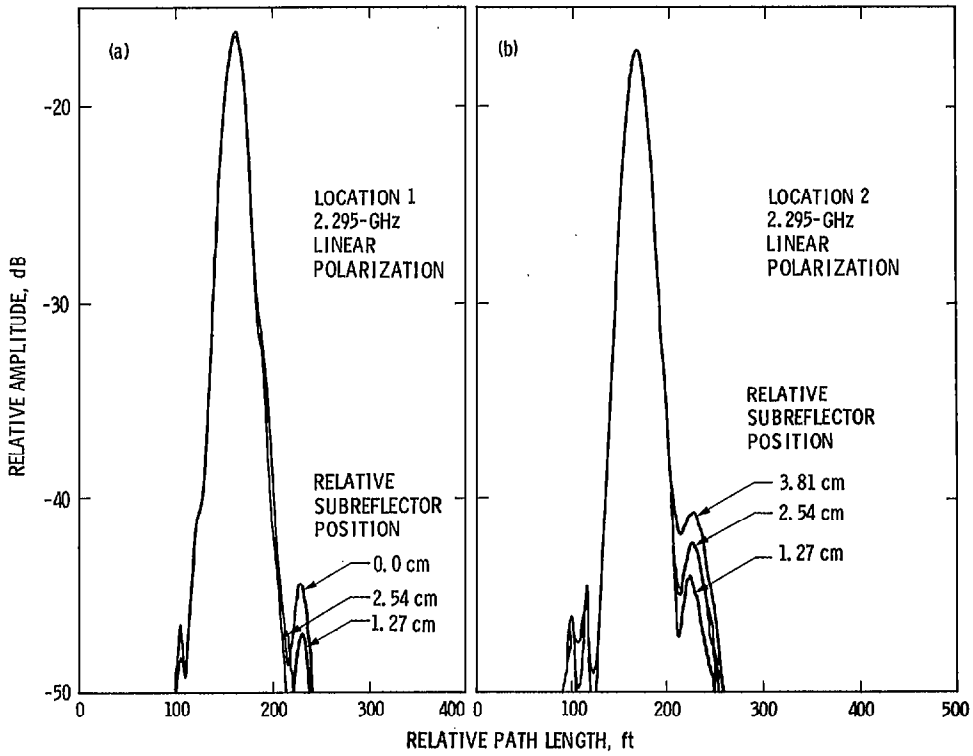

Fig. 10. Sample recordings of path lengths and signal magnitudes of primary and secondary signals for a 26-m antenna test setup with the transmit horn located (a) close to side of cone housing and (b) near the edge of paraboloid. To convert horizontal scale to absolute path length for either plot, subtact the reference path length measurement of 95 ft.